Waste Management 144 (2022) 376–386

Contents lists available at ScienceDirect

Waste Management

journal homepage: www.elsevier.com/locate/wasman

Country report

Co-conversion of wood and polyvinyl chloride to valuable chemicals and high-quality solid fuel

Xiaolin Chen, Xianglan Bai *

Department of Mechanical Engineering, Iowa State University, Ames, IA, USA

ARTICLE INFO

Keywords:
PVC
Wood
Levoglucosenone
Furfural
5-Chlorovaleric acid
Hydrogen chloride

ABSTRACT

Polyvinyl chloride (PVC)-containing waste streams are difficult to recycle due to high chlorine content in PVC. Toxic dioxins or corrosive hydrogen chloride (HCl) vapor released from improper management of PVC-containing wastes can cause severe environmental pollution and human health problems. While PVC is usually treated as contamination and burden in waste recycling, a novel recycling approach was developed in this study to leverage PVC as an asset. Specifically, red oak and PVC were co-converted in γ-Valerolactone, a green biomass-derivable solvent. During the co-conversion, PVC-derived HCl in the solvent acted as an acid catalyst to produce up to 14.4% levoglucosenone and 14.3% furfural from red oak. On the other hand, dechlorinated PVC hydrocarbons and lignin fraction of red oak reacted each other to form chlorine-free solid fuels with high thermal stability. The higher heating value of the solids was up to 36.2 MJ/kg, which is even higher than the heating value of anthracite coal. After the co-conversion, more than 80% of PVC-contained chlorine turned into chloride ion and the rest formed 5-chlorovaleric acid. 5-chlorovaleric acid crystals were further recovered from the post-reaction liquid with a purity of 91.2%.

1. Introduction

In 2018, 292.4 million tons of municipal solid wastes (MSW) were generated in the US alone. Of which, less than half of MSW were recycled or combusted for heat and the rest were sent to landfills (EPA, 2021). The landfilled wastes not only caused significant environmental issues but also brought economic burdens associated with waste transportation and the maintenance of landfill sites (Kollikkathara et al., 2010; Mukherjee et al., 2014; Danthurebandara et al., 2015; Vaverková, 2019). The landfilled materials consisting of organics and synthetic polymers also represent tremendous energy and resource losses (Kumar and Sharma, 2014; Srivastava and Chakma, 2020). While proactive measurement has been taken in recent years to increase the recycling rate, effective waste recycling has yet been developed. The ease of recycling largely depends on the type and form of the waste materials. Clean plastics are usually considered for mechanical recycling, and organic wastes could be composed for fertilizers (Polprasert, 2007; Schyns and Shaver, 2020). Plastic wastes such as polyethylene terephthalate, polystyrene, polyurethane, polyamide can also be chemically recycled to monomers that are useful in chemical synthesis (Xue et al., 2017; Raheem et al., 2019; Queiroz et al., 2020; Thiounn and Smith, 2020; Jiang et al., 2022; Song et al., 2022). Co-mingled and/or contaminated wastes are usually much more difficult to recycle due to their heterogeneous composition and the release of pollutants during the recycling processes (Chen et al., 2021). Other than incineration for heat, various strategies have been developed to convert mixed waste materials into liquid fuels, syngas, or chemicals by employing pyrolysis, gasification, and solvent-based conversion approaches (Arena, 2012; Chen et al., 2021; Hameed et al., 2021; Wang et al., 2021). For example, co-pyrolyzing biomass and polyolefins plastics can increase the heating value of bio-oil, and synergistically enhance hydrocarbon production during catalytic pyrolysis, which are attributed to the hydrogen donating effect of polyolefins (Xue et al., 2015; Xue et al., 2016; Xue and Bai, 2018).

PVC-containing wastes are considered the most challenging materials to recycle. PVC is widely used in construction, household items, electronics, and medical devices due to its durability, corrosion resistance, and low cost (Titow, 1999). However, PVC is also the major halogen source in the waste streams as about 57 wt% of the polymer mass is made of chlorine element. Chlorinated dioxins produced during PVC combustion are highly toxic to human health: skin disease can be caused by short-term exposure to dioxins, while chronic exposure to

* Corresponding author.
E-mail address: bxl9801@iastate.edu (X. Bai).

https://doi.org/10.1016/j.wasman.2022.04.018
Received 8 December 2021; Received in revised form 15 February 2022; Accepted 12 April 2022
Available online 19 April 2022
0956-053X/© 2022 Elsevier Ltd. All rights reserved.

dioxins can cause cancer (Braun, 2002; Sadat-Shojai and Bakhshandeh, 2011; Zhang et al., 2015). Additionally, the chloride in the atmosphere also leads to acidic rain. Thus, PVC dechlorination prior to incineration is usually required. During waste recycling, the presence of PVC in the waste materials also causes various detrimental effects. It was reported that PVC in its mixture with biomass reduced tar cracking efficiency and caused catalyst poisoning during gasification (Huang et al., 2016). It was also found that co-pyrolysis with PVC and other waste materials increased char yield and produced chlorine-contaminated bio-oil and char (Zhou et al., 2015). Even landfilling is not suitable for PVC as oxidative degradation of PVC can occur under natural exposure (Decker, 1976; Decker, 1984; Krzymien, 1997). So far, a variety of PVC dechlorination technologies have been studied. A stepwise pyrolysis was performed on the mixture of PVC, polystyrene (PS), and polyethylene (PE), where PVC-derived HCl was removed in the first stage, and styrene and aliphatic compounds were formed in the later stages (Bockhorn et al., 1999). Various absorbent materials were also used to trap the PVC-released HCl physically or chemically. Previously, PVC was ball-milled with alkali (KOH or NaOH) pellets to remove chlorine by forming chloride salts (Inoue et al., 2005). Petroleum residue was also used to absorb chlorine during PVC pyrolysis because the asphaltenes of petroleum residue could react with chloride radicals evolved from PVC cracking before the formation of HCl (Ali and Siddiqui, 2005). An Al-Zn composite catalyst was used as both cracking catalyst and dechlorination agent during plastic conversion, where the evolved HCl was fixed onto the catalyst and thus the chlorine content in the oil was reduced (Tang et al., 2003). Co-pyrolysis of demolition wood and PVC film was previously investigated (Kuramochi et al., 2008). In the study, the decreased HCl emission during co-pyrolysis was accompanied by the production of chlorine-contaminated bio-oil and char. A hydrothermal carbonization of PVC-containing medical wastes and biomass was also investigated (Shen et al., 2017). While the dissolution of HCl in water prevented the release of the corrosive vapor, up to 32% of chlorine ended up in the solid products. In a recent study, waste PVC containing high content of plasticizers was converted using a critical aqueous ammonia process to produce a chlorine-free oil and an aqueous product containing inorganic chloride (Xiu et al., 2020). Overall, recycling PVC-containing waste streams remains as a challenging task. The previous approaches for PVC dechlorination often generated toxic and corrosive vapors, chlorine-contaminated oil, solids, or catalysts, which can potentially serve as secondary pollution sources.

In this work, a novel recycling method was explored to convert the mixture of PVC and wood. Wood wastes are generated from various sources and are available in different forms (Shahidul et al., 2020; Cesprini et al., 2020; Tamanna et al., 2020). While wood and PVC are both major MSW components, they co-present in construction and demolition wastes in considerable amounts. Manually sorting PVC from the co-mingled waste streams is costly. Furthermore, wood-PVC composites are also impossible to sort mechanically. As a result, the unsorted wood and PVC are generally sent to landfills (Helsen and Van den Bulck, 2005; Kim et al., 2020; Sadat-Shojai and Bakhshandeh, 2011).

In a previous work, we reported that when cellulose and PVC were co-processed in a polar aprotic solvent, PVC decomposition started ahead of cellulose conversion. As a result, cellulose depolymerization was promoted by PVC-derived HCl dissolved in the solvent (Braden and Bai, 2018). Encouraged by the previous result, co-conversion of wood and PVC in solvent was investigated in this study. Unlike conventional recycling approaches where PVC was contaminant and burden, the presented approach leveraged the chemical composition of PVC and its unique thermal decomposition properties as advantages to co-produce valuable chemicals and high-quality clean solid fuel.

2. Experimental

2.1. Materials

Red oak was purchased from Wood Residues Solutions (Montello, WI) and ball-milled to a particle size of 250 ~ 400 μm. Ultimate, proximate, and compositional analysis results of red oak are given in Table S1 in the supporting information (A et al., 2021). PVC powders were purchased from the Shanghai Yangli Mechanical and Electrical Technology Co., Ltd, China. Elemental composition of PVC is given in Table S2. The chlorine content in the PVC material is 56.61 wt%, due to its high purity. γ -Valerolactone (GVL) with a 98% purity was purchased from Fisher Scientific. Levoglucosenone (LGO) and levoglucosan (LGA) were purchased from GlycoSyn. Furfural (FF) and 5-chlorovaleric acid (CA) were purchased from Sigma Aldrich.

2.2. Conversion in solvent

The solvent-based conversion was conducted using mini stainless-steel batch reactors with an inner volume of 3 mL. For each experiment, 12 mg of red oak and different amounts of PVC were added to 2 mL GVL. The reactors were heated using a fluidized sand bath. When the preset temperatures were reached, the reactors were dropped into the sand bath to start reactions. After reaction times were reached, the reactors were quickly removed and quenched in a water bath at ambient temperature.

After the reactions, the liquid and solid suspensions were extracted from the reactor using glass syringes and separated by 0.45 μm glass fiber filters. The liquid-removed solid residues were then thoroughly washed using water and dried in a 40 °C vacuum oven overnight. For all the cases, the gas production was negligible. Thus, the yields of liquid and solid residue were determined according to the equations given below:

$$Solid\ \ residue\ \ yield\ \ (\%) = \frac{mass\ \ of\ \ solid\ \ residue}{mass\ \ of\ \ red\ \ oak\ \ plus\ \ PVC}$$

$$\text{Liquid yield } (\%) = 100\% - solid\ \ residue\ \ yield\ \ (\%)$$

2.3. GC–MS analysis

The liquid products were analyzed using an Agilent 7890B Gas Chromatograph (GC) equipped with Mass Spectrometer (MS) and Flame Ionization Detector (FID). Two ZB-1701 (60 m × 250 μm × 0.25 μm) capillary columns were used. The GC oven temperature was first held at 40 °C for 3 min, further elevated to 280 °C at 4 °C/min, and then held at 280 °C for another 4 min. Helium was used as the carrier gas with a 1 mL/min flow rate and a split ratio of 20:1 at the GC inlet. The monomers were identified by MS and quantified by FID. Calibrations were performed using standard chemicals. The yields of biomass-derived compounds (i.e., LGO, FF) were reported based on the red oak mass.

2.4. Solvent pH

The acidity of the reaction solution was determined using a pH meter (Mettler Toledo SevenMulti pH meter). Each test was repeated five times, and average values were reported.

2.5. FTIR analysis

FTIR analysis of solid samples was performed using a Thermo Scientific Nicolet iS10 (Thermo Fisher Scientific Inc., Waltham, MA) equipped with a Smart iTR accessory. The wavenumbers ranged from 750 cm^{-1} to 4000 cm^{-1}. Each sample was scanned 32 times at a resolution of 4 cm^{-1} and an interval of 1 cm^{-1}.

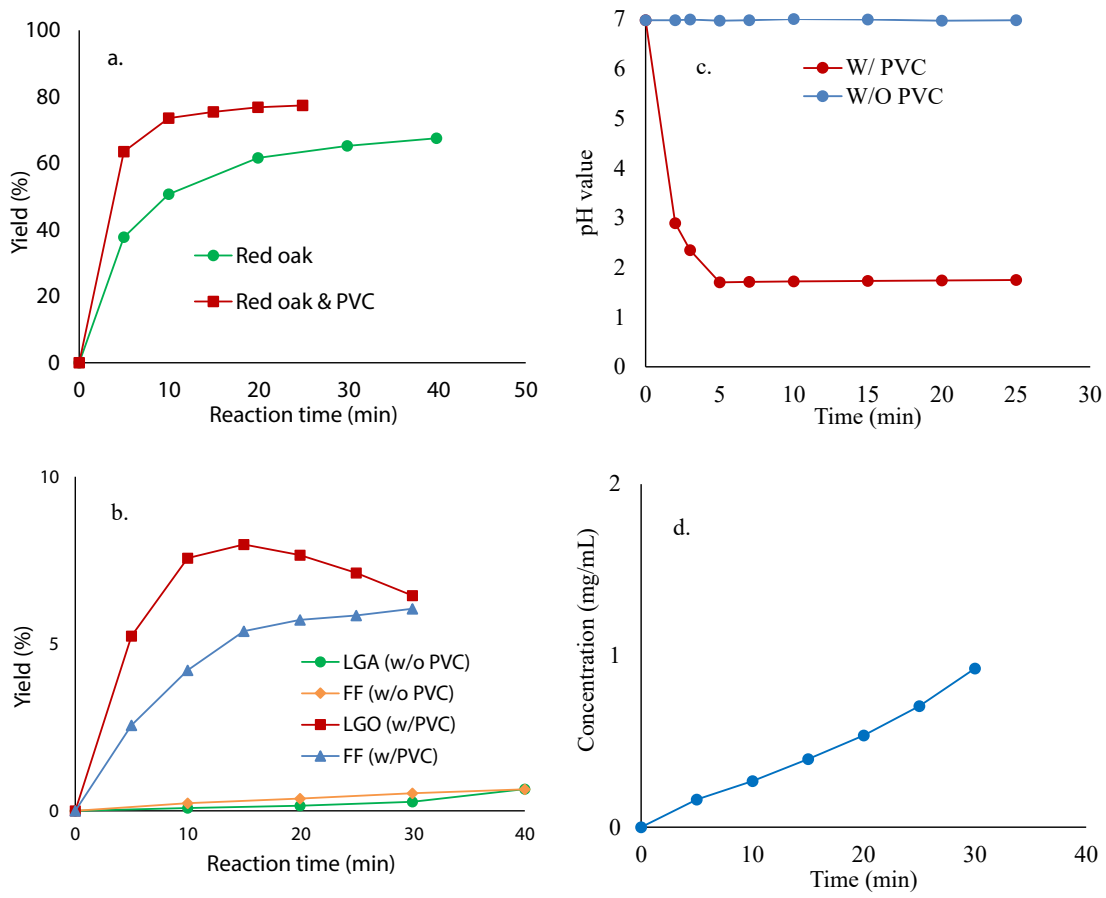

Fig. 1. Comparison of red oak conversion in 280 °C GVL with and without PVC (a 2:1 ratio of red oak to PVC). a. liquid yield; b. red oak-derived monomer yields; c. solution pH; d. CA concentration in reaction solution, as function of reaction time. (For interpretation of the references to color in this figure legend, the reader is referred to the web version of this article.)

2.6. Thermogravimetric (TGA) analysis

TGA analysis of solid samples was conducted using a Mettler Toledo Thermogravimetry/Differential Scanning Calorimetry system (TGA/DSC). The sample was heated from ambient temperature to 900 °C at 10 °C/min. Nitrogen gas with a flow rate of 100 mL/min was used as the environment gas.

2.7. Fast pyrolysis

Fast pyrolysis of solid samples was conducted using a micro-pyrolyzer system (Rx-3050 TR, Frontier Laboratory, Japan). Around 250 μg of the sample was pyrolyzed at 500 °C using helium as the environment gas. The pyrolysis vapors were swept into the online GC/MS-FID for instant analysis. At the front inlet of GC, the flow rate of helium was 156 mL/min and the split ratio was 50:1. The GC heating profile was described above.

2.8. SEM analysis

The microstructure of solid samples was examined using a scanning electron microscope (SEM, Quanta-FEG 250, FEI) and an accelerating voltage of 10 kV. Segments of the samples were mounted onto a double-stick carbon tape on a 45° incline and coated with 5 nm of iridium for conductivity.

2.9. Elemental analysis

Elemental analysis of solid samples was performed using a CHNS Elemental Analyzer (Vario Micro Cube). Carbon, hydrogen, and nitrogen contents were measured, and oxygen content was calculated by mass difference. The higher heating value (HHV) was obtained by using Dulong's Formula.

2.10. Chlorine determination

The total chlorine content in solid samples was determined using the oxidative combustion titration method (i.e., method 9076). Initially, the solid was fully combusted inside the sealed apparatus. Deionized (DI) water was then added to the apparatus through a valve on the apparatus to absorb the combustion products. After the combustion smoke was fully absorbed, a few drops of K_2CrO_4 were added to the solution as an indicator. In the following process, $AgNO_3$ was added dropwise to the solution to precipitate chloride ion as AgCl until the color of the solution suddenly changed due to the Ag_2CrO_4 formation after the complete precipitation of chloride in the solution. The chlorine in the solid was calculated based on the added amount of $AgNO_3$. CA was quantified using the standard chemical in GC/MS.

2.11. Recovery of CA

After the solid products were separated by filtration, DI water was added to the post-reaction liquids in an ice bath to precipitate CA. The precipitate was filtered and then thoroughly washed using water. Finally, the precipitate was dissolved in methanol and analyzed using GC/MS-FID.

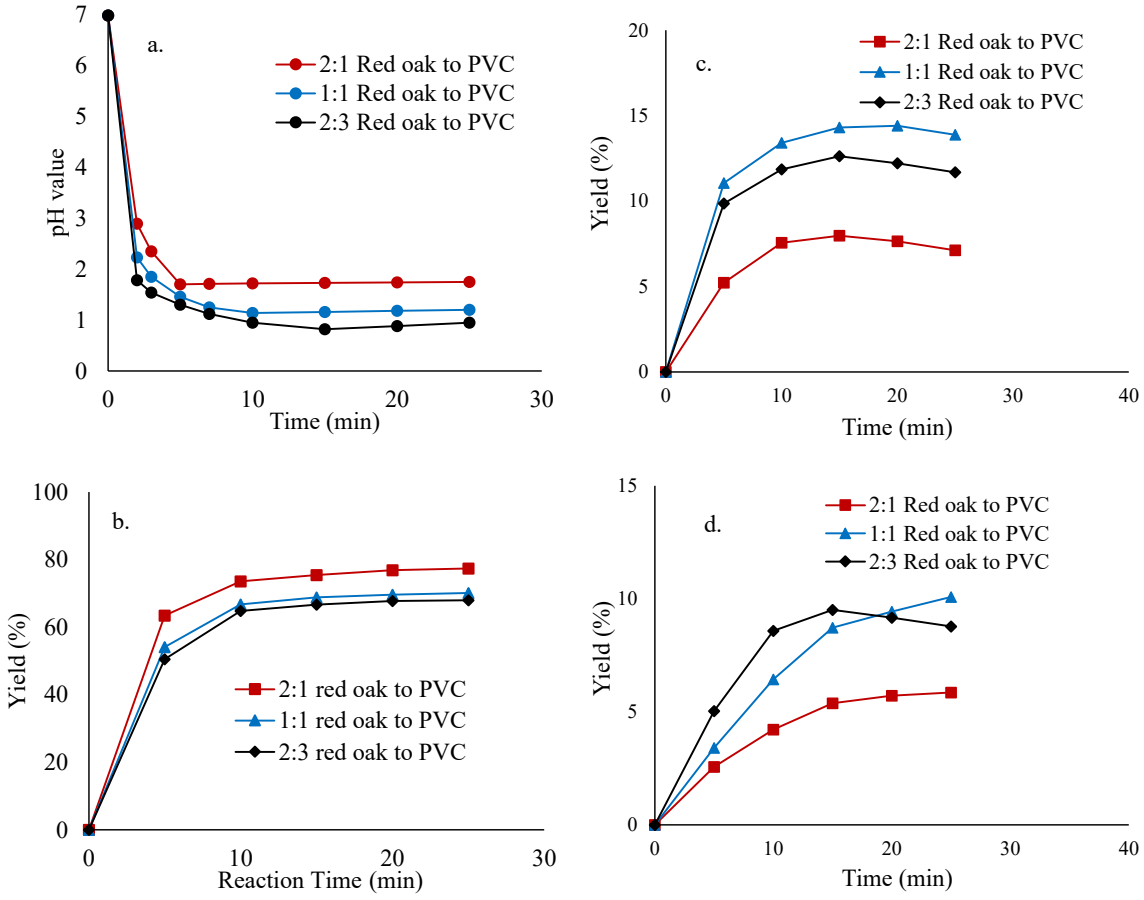

Fig. 2. The effect of PVC loading. a. solution pH value; b. liquid yield; c. LGO yield; d. FF yield, as function of reaction time.

3. Results and discussions

3.1. Co-conversion of red oak and PVC in GVL

3.1.1. Effect of PVC

Red oak was converted in 280 °C GVL alone, or in the presence of PVC (a 2:1 red oak to PVC ratio). The results are given in Fig. 1. Without PVC, the liquid yield was 50.6% after a 10 min reaction and it increased to 67.5% at 40 min (Fig. 1a). Polar aprotic solvents, such as GVL, can reduce the activation energy of glycosidic bond dissociation to depolymerize cellulose and hemicellulose into soluble carbohydrates with shorter chain lengths while also dissolving lignin (Ghosh et al., 2016). Both the liquid yield and liquefaction rate were higher when red oak was co-converted with PVC. With PVC, the liquid yield reached 73.6% at 10 min. Further increasing reaction time only slightly promoted the liquid yield to obtain 77.4% at 25 min.

As shown in Fig. 1b, monomers were barely produced from red oak in the absence of PVC. Only up to 0.7% of FF and 1.0% LGA were detected in the liquid. Without a catalyst, the reaction condition was too mild to depolymerize the cellulose chain into monomers. In comparison, LGO and FF were two major monomers produced from red oak when PVC was co-converted. LGO yield at 10 min was 7.6% and increased to 8.0% at 15 min before it leveled off. The leveling off in LGO yield at the prolonged reaction is due to degradation and other secondary reactions of LGO. FF yield was 4.2% and 5.7% at 10 min and 20 min, respectively. LGO is one of the top value-added biobased chemicals. It has a variety of applications in organic synthesis, such as asymmetric synthesis, enantiospecific synthesis, and medicinal chemistry (Zanardi and Suárez, 2009; M. Sarotti et al., 2012; Comba et al., 2017). LGO is a double dehydrated anhydroglucose. In previous studies, LGO was produced by converting cellulose or cellulosic biomass in the presence of acid catalysts (Cao et al., 2015; He et al., 2017; Wei et al., 2014; Hu et al., 2020). During acid-catalyzed decompositions of cellulose, LGA can serve as a precursor of LGO. FF is an important platform chemical, which has wide applications in plastics, and pharmaceutical and agrochemical industries. It is a natural precursor to a range of furan-based chemicals and solvents (Dias et al., 2010; Eseyin and Steele, 2015; Kabbour and Luque, 2020). FF is also a dehydration product of carbohydrates (Ghosh et al., 2016). While FF can also be produced from cellulose, it is mainly derived from hemicellulose when biomass is converted (Mamman et al., 2008). Similar to LGO, FF production from biomass is also promoted by acid catalysts (Machado et al., 2016; Ghosh et al., 2018). In this study, noticeable amounts of LGO and FF were obtained from red oak in the presence of PVC although no acid catalyst was added to the reaction solution.

Thermal decomposition of PVC usually starts from dehydrochlorination of PVC polymer chain to form HCl, which is followed by cyclization and aromatization of dechlorinated polyene to form aromatics (Stromberg et al., 1959). Thus, it is possible that the *in-situ* generated HCl served as an acid catalyst to promote red oak decomposition during the co-conversion of red oak and PVC. Nevertheless, such catalytic activities by HCl are possible only when dehydrochlorination of PVC is fast enough that it proceeds ahead of red oak decomposition (Braden and Bai, 2018). Since the release of HCl would increase the solution acidity, PVC dehydrochlorination and its rate could be evaluated by monitoring the solution pH during the co-conversion of red oak and PVC. As given in Fig. 1c, the solution pH remained at near 7 with increasing reaction time when red oak alone was converted in GVL. When PVC was co-converted, the pH value dropped from 7 to 1.7 within the initial 5 min, which confirms the rapid PVC dehydrochlorination and the dissolution of HCl

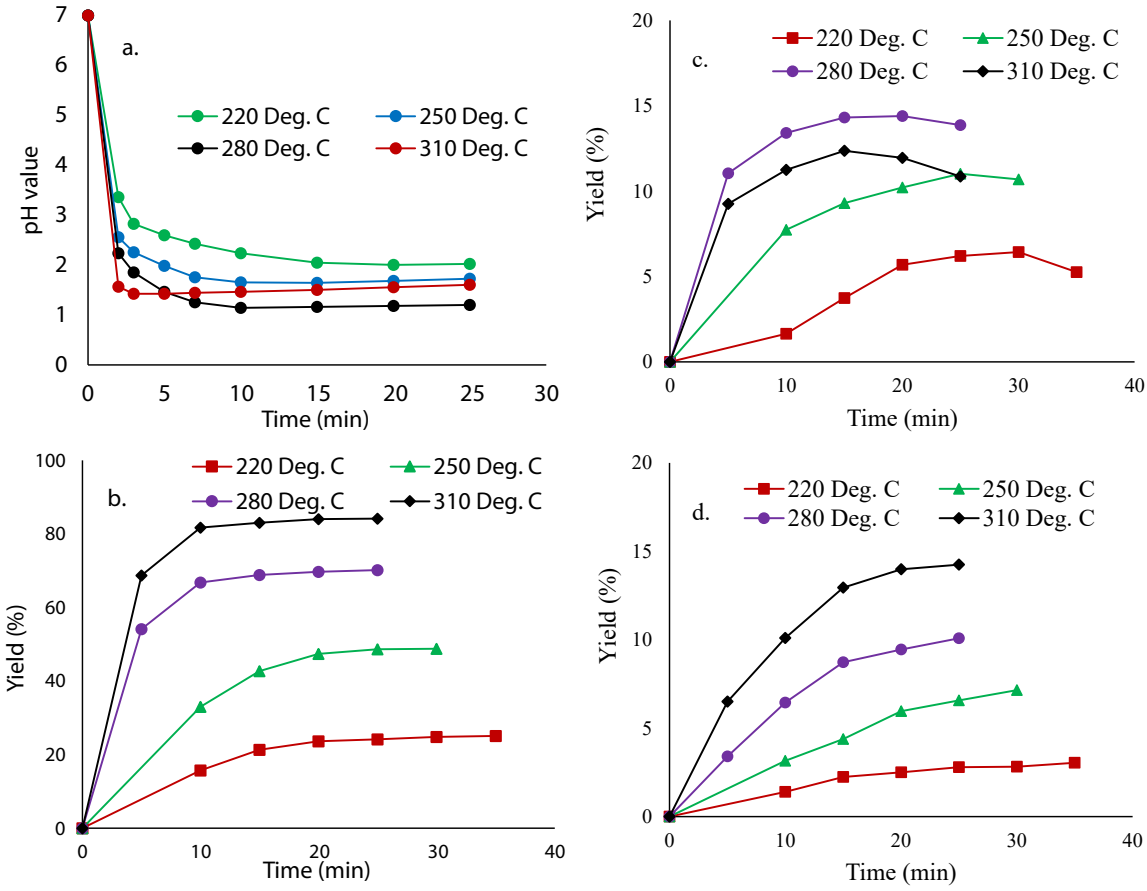

Fig. 3. The effect of solvent temperature. a. solution pH; b. liquid yield; c. LGO yield; d. FF yield, as function of reaction time.

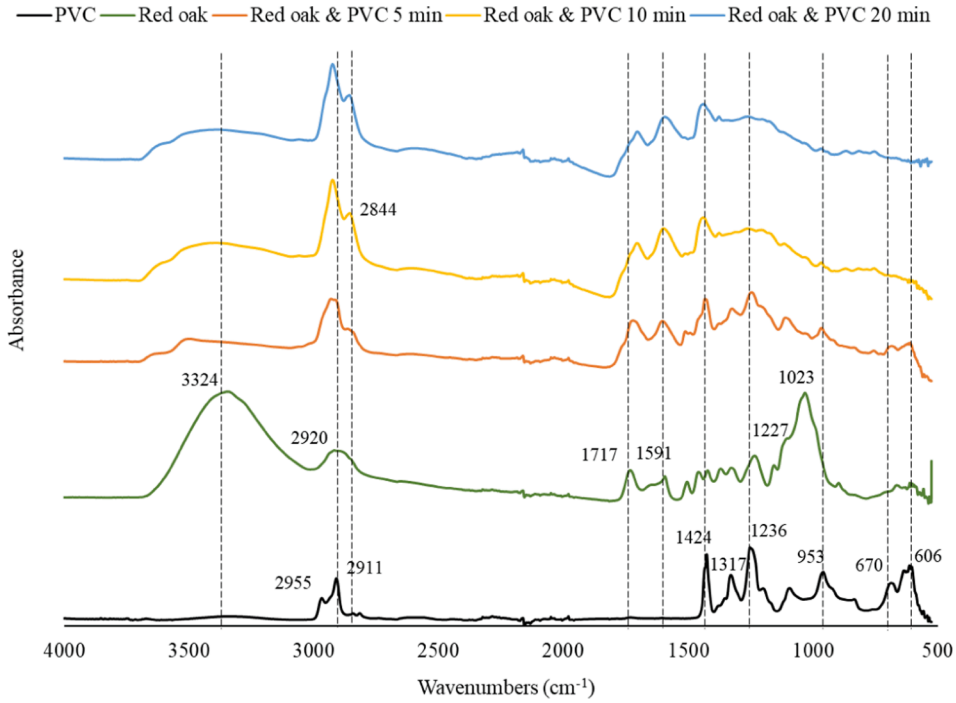

Fig. 4. FTIR spectra of PVC, red oak, and the solids recovered during co-conversion of a 1:1 ratio of red oak and PVC in 280 °C GVL for various reaction times. (For interpretation of the references to color in this figure legend, the reader is referred to the web version of this article.)

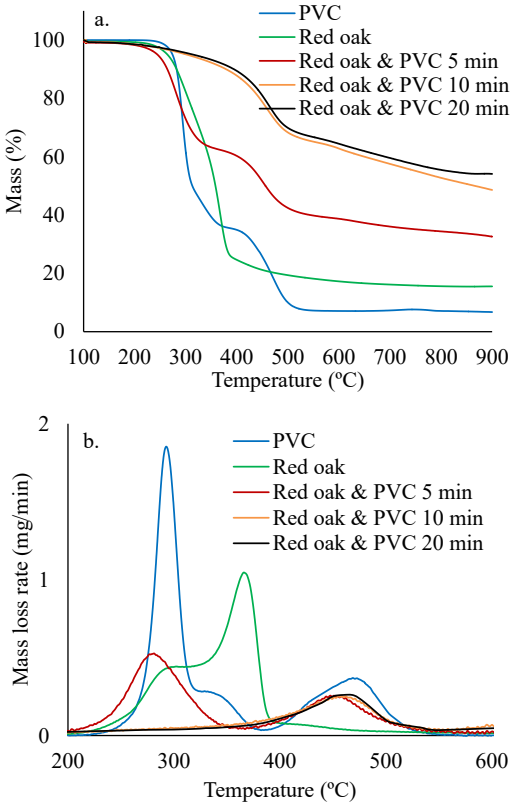

Fig. 5. TGA results of PVC, red oak and the solids recovered during co-conversion of a 1:1 ratio of red oak in 280 °C GVL for various reaction times. a. TGA; b. DTG. (For interpretation of the references to color in this figure legend, the reader is referred to the web version of this article.)

in the solvent. No further decrease of the pH value was observed after 5 min. Instead, the solution pH slightly increased with increasing reaction time to become 1.75 at 25 min. The reversed trend of the solution pH after 5 min was due to the formation of CA and its increased concentration in the reaction solution along with increasing reaction time (Fig. 1d). CA is a secondary reaction product of HCl, formed when HCl reacts with GVL to attach its H and Cl onto the opened furan ring of GVL. The result suggests that PVC dehydrochlorination mostly completed within the first 5 min, and the transition from HCl to less acidic CA reduced the HCl content in the reaction solution to increase the pH value.

3.1.2. *Effect of PVC loading*

As shown above, valuable chemicals were produced from red oak catalyzed by HCl in the solution. Since HCl is *in-situ* generated during PVC decomposition, its concentration in the reaction solution would depend on both the dehydrochlorination rate of PVC and PVC loading. The effect of PVC loading was investigated by co-converting a fixed amount of red oak with different amounts of PVC in 280 °C GVL. The results are given in Fig. 2. As shown in Fig. 2a, the solution pH became lower with increasing PVC loading because a larger amount of HCl would be produced from a higher PVC loading. It was also found that the reaction time required for the solutions to reach the minimum pH values increased with increasing PVC loading. The minimum pH values of the solutions were 1.7, 1.14, and 0.82 in the cases of the red oak to PVC ratios of 2:1, 1:1, and 2:3, reached at 5 min, 10 min, and 15 min, respectively. This is because a longer reaction time would be needed to complete PVC dehydrochlorination with a higher PVC loading. After the minimum values were achieved, the solution pH increased with increasing reaction times for all the cases. This trend was more noticeable with a higher PVC loading, which corresponds to the higher transition from HCl to CA with increasing PVC loading, as shown in Figure S1.

Increasing PVC loading resulted in decreased liquid yields (Fig. 2b) and increased solid yields (Figure S2). The liquid yield obtained using a 25 min reaction time was 77.4%, 70.2%, and 68%, respectively, when the red oak to PVC ratio to be 2:1, 1:1, and 2:3. In Fig. 2c, overall higher LGO yields were produced using a 1:1 ratio of red oak to PVC. The maximum LGO yield of 14.4% was obtained after a 20 min reaction, which is equivalent to 35% per cellulose in red oak. In comparison, the optimal LGO yield was 8.0% and 12.6% by using 2:1 and 2:3 ratios of red oak to PVC, respectively. While acid catalyzes LGO formation, an excessive amount of acid in the solution can also cause LGO degradation or other competing reactions. For example, LGO could convert to FF in the presence of water byproduct resulted from red oak dehydration (Kawamoto et al., 2007). In Fig. 2d, FF production was promoted by increasing PVC loading. On the other hand, FF became increasingly unstable for the case of 2:3 red oak to PVC ratio due to the highest PVC loading, and as a result, FF yield decreased with increasing reaction time after it reached 9.5% at 15 min. FF was thermally more stable with lower PVC loadings. The highest FF yield of 10.1% was obtained for the case of a 1:1 red oak to PVC ratio after a 25 min reaction.

3.1.3. *Effect of solvent temperature*

The effect of solvent temperature was investigated by co-converting a 1:1 ratio of red oak and PVC and varying solution temperatures between 220 °C and 310 °C. The results are given in Fig. 3. The rate of PVC dehydrochlorination was enhanced by increasing solvent temperature, evident by the steeper drops of the solution pH at the initial stage (Fig. 3a). The pH value of the solution measured after a 3 min reaction was 2.82, 2.25, 1.85, and 1.42, respectively, with the solvent temperatures of 220, 250, 280, and 310 °C. After 3 min, the solution pH started to increase along with increasing reaction time for the 310 °C case whereas it further decreased for the other lower temperature cases. The minimum pH value and the corresponding reaction time were 1.14 and 10 min for the 280 °C case and 1.64 and 15 min for the 250 °C case. For the 220 °C case, the solution pH decreased monotonically to reach 2.0 at 25 min, likely due to slow dehydrochlorination of PVC by using the low temperature. As given in Figure S3, CA concentrations in the reaction solutions were higher and also increased faster with increasing solvent temperatures. Due to the increased transition of HCl to CA at higher temperatures (Figure S3), the solution pH for the 310 °C case was overall higher than that for the 280 °C case.

Increasing solvent temperature accelerated the liquefaction rate and enhanced liquid yield (Fig. 3b). The maximum liquid yield of 84.1% was achieved by using a solvent temperature of 310 °C and a reaction time of 25 min, compared to 25.4% obtained during the co-conversion at 220 °C for 40 min. The solvent temperature and solution acidity are both important parameters affecting biomass conversion. Although the solution acidity was lower than the case of 280 °C, red oak liquefaction was highest with the case of 310 °C. Thus, the effect of solvent temperature on liquid yield was greater than the effect of solution acidity in this study. As shown in Fig. 3c, increasing solvent temperature to 280 °C accelerated LGO production and shortened the optimal reaction time. Compared to the maximum LGO yield of 14.4% obtained for the 280 °C case, the optimal yield with the 310 °C case was 12.4% although it was still higher than 10.9% obtained for the 250 °C case. LGO yield was lowest for the 220 °C case where PVC dehydrochlorination was the slowest and the most incomplete in this study. Thus, the order of the increasing LGO production well corresponds to the order of increasing solution acidity at different solvent temperatures. On the other hand, FF yield monotonically increased with increasing solvent temperature and reaction time in Fig. 3d. The highest FF yield of 14.3% was achieved for the 310 °C case at 25 min.

Fig. 6. SEM results. a-c. red oak; d-f. red oak alone converted in 280 °C GVL for 40 min; g-i. the solid recovered by co-converting a 1:1 ratio of red oak and PVC; j-l. the solid recovered by co-converting a 2:3 ratio of red oak and PVC. In g-l, the solvent temperature is 280 °C and the reaction time is 20 min. (For interpretation of the references to color in this figure legend, the reader is referred to the web version of this article.)

3.2. Evaluation of solid product

3.2.1. FTIR analysis results

While LGO and FF were derived from carbohydrates of red oak, lignin-derived products were barely observed during the liquid analysis. Only trace amounts of phenolics were observed, which are 3,5-dimethoxy-4-hydroxycinnamic acid, 2′,4′-Dimethoxyacetophenone, and 2,6-dimethoxy-4-(2-propenyl)-phenol. PVC-derivable chlorinated or dechlorinated hydrocarbons were also not found in any of the liquids. Therefore, the solid products were also characterized to investigate their origin. FTIR spectra of the solids recovered at different reaction times using a 1:1 ratio of red oak to PVC and a solvent temperature of 280 °C are given in Fig. 4. The FTIR results of PVC and untreated red oak are also included as references.

For PVC, the bands at 606 and 670 cm^{-1} are associated with C-Cl stretching in -CHCl groups. The bands at 2911 and 2955 cm^{-1} originate from aliphatic C-H. The band at 1424 cm^{-1} is due to C-H in CH_2, and the band at 1236 cm^{-1} is for C-H bending at -CHCl. In addition, the band at 953 cm^{-1} is for C-H wagging. For red oak, the broad band at the 3200–3600 cm^{-1} region represent O-H stretching. The broad band centered at 2920 cm^{-1} is for methyl and ethyl C-H and, and the 1717 cm^{-1} band corresponds to C=O bonds. The band at 1591 cm^{-1} is for aromatic ring vibration, which is caused by lignin structure. The band at 1227 cm^{-1} is for aryl-alkyl ether linkage (C-O-C), and the 1023 cm^{-1} band is for C-O-H mainly originating from carbohydrates. In addition to the red oak-originating bands, the PVC chlorine-associated bands (606, 670, 1236 cm^{-1}) and PVC hydrocarbon-associated bands (1424, 1317, ~2903 cm^{-1}) were also observed in the solid recovered after a 5 min co-conversion of red oak and PVC. Therefore, PVC dehydrochlorination was incomplete at the given reaction time. In comparison, the chlorine-related bands completely disappeared at the solids recovered after 10 and 20 min of the co-conversion, suggesting the solids were dechlorinated. Compared to untreated red oak, the 3200–3600 cm^{-1} and 1023 cm^{-1} bands largely decreased in all the solids. Their decreases correspond to the removal of carbohydrates from red oak during the co-conversion. On the other hand, the alkyl C-H related bands at 2920,

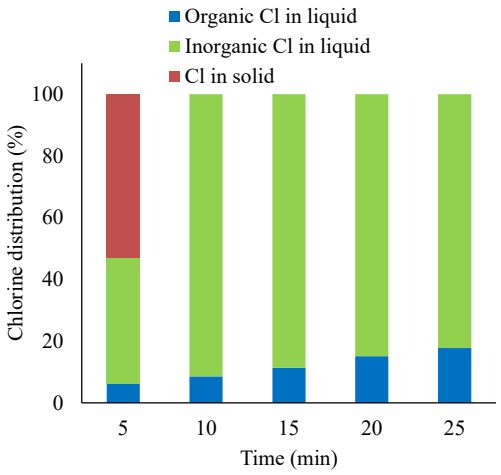

Fig. 7. Distribution of chlorine in liquid and solid products during co-conversion of a 1:1 ratio of red oak and PVC in 280 °C GVL. (For interpretation of the references to color in this figure legend, the reader is referred to the web version of this article.)

2844, and 1424 cm^{-1} were strongly enhanced in all the solids, which are contributed by PVC-originated hydrocarbons. In addition, the bands at 1717 cm^{-1} for C=O and 1591 cm^{-1} for the aromatic ring are also the major bands in the solids recovered at 10 and 20 min. Thus, the FTIR results suggest that during co-conversion of red oak and PVC, the dechlorinated PVC hydrocarbons and the lignin fraction of red oak formed the solid products. Dehydrochlorinated PVC hydrocarbons can be highly reactive due to the formations of radicals and unsaturated C=C bonds. During the co-conversion of red oak and PVC, the polyenes and hydrocarbon radicals can readily react with lignin or fragmented lignin molecules to form solid products. The features of the bands at below 1400 m^{-1} were largely weakened in the solids recovered at 10 or 20 min, implying the solids have highly condensed structures.

3.2.2. TGA analysis results

The TGA profiles of the solids (a 1:1 ratio of red oak to PVC, 280 °C) obtained at different reaction times are compared with PVC and untreated red oak in Fig. 5. The T_d (i.e., the temperature for 5% mass loss) and the residue mass at 900 °C are also given in Table S3 for the tested samples. Thermal decomposition of PVC proceeded via two-stages in Fig. 5a, which include dehydrochlorination at lower temperatures, and cyclization and aromatization of polyene to form aromatic compounds at higher temperatures.

In Fig. 5b, the first DTG peak of PVC appearing at around 300 °C is due to HCl release. The shoulder peak at its right side is due to the release of HCl, benzene, and a minor amount of condensed aromatic hydrocarbons. The second DTG peak appearing at 400–550 °C is due to the volatilization of alkylbenzenes, such as toluene and xylene, and polyaromatic hydrocarbons, such as naphthalene, which are produced from inter- and intramolecular condensations (McNeill et al., 1995; Yu et al., 2016). Red oak decomposes at a much broader temperature range than PVC due to its complex composition. Usually, hemicellulose decomposes first (i.e., the shoulder DTG peak at around 320 °C) followed by cellulose decomposition (i.e., the major DTG peak at 380 °C). Lignin is highly recalcitrant toward thermal decomposition, and thus can decompose at up to 900 °C (Brebu and Vasile, 2010). Lignin is also the main contributor of solid residue when biomass is pyrolyzed. In Fig. 5b, two DTG peaks were observed with the solid recovered at 5 min. The first DTG peak corresponds to the volatilization of PVC-derived HCl, indicating PVC dehydrochlorination was incomplete at the given reaction time. On the other hand, the shoulder DTG peak that appeared in pure PVC was not observed in this solid, whereas the higher temperature (400–550 °C) DTG peak of PVC remained. Thus, it is unlikely that intact PVC polymer remained in the solid although PVC dehydrochlorination was incomplete at this stage of the co-conversion. The DTG peak corresponding to the HCl volatilization disappeared in the solids recovered at 10 and 20 min, confirming the complete dehydrochlorination of PVC at the given conditions. The TGA results also well match the FTIR results of the solids described above. Only one DTG peak appeared at 400–550 °C in the solids recovered at 10 and 20 min, implying they are

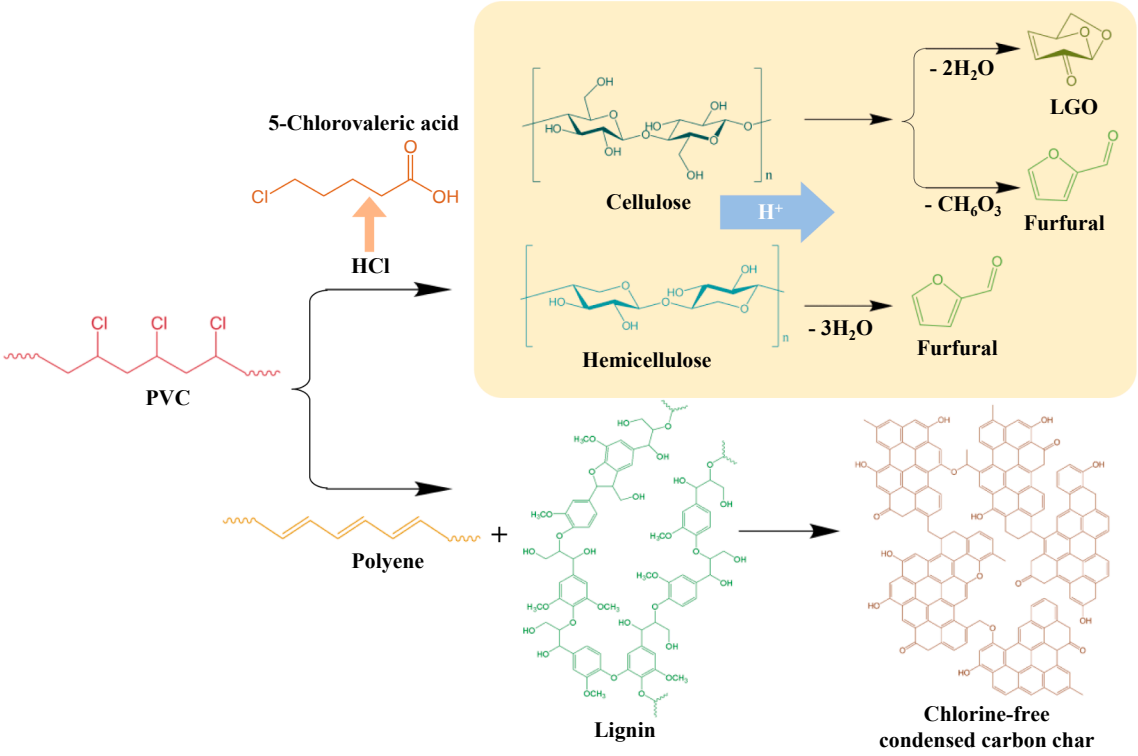

Fig. 8. Proposed reaction pathway.

thermally much more stable than PVC or red oak. Due to their condensed structures, up to 54% char remained at 900 °C when these solids were pyrolyzed.

3.2.3. Pyrolysis of solid products

In this study, the solids remaining after the co-conversion in GVL were also fast pyrolyzed and the volatilizable products were identified using GC/MS. Since fast pyrolysis causes bond cleavages in the solids, the information about the original chemical structures of the solids can be obtained by analyzing the pyrolysis products. The GC/MS chromatograms obtained during pyrolysis of the solids are given in Figure S5. Carbohydrate-derived compounds were not observed, confirming carbohydrates of red oak were completely converted and removed from the solid. HCl was observed when the solid recovered at 5 min was pyrolyzed, which agrees with the above-described results of TGA and FTIR. Additionally, PVC-derived benzene, naphthalene, and alkyl aromatic hydrocarbons were also observed among the pyrolysis products. In comparison, neither HCl nor organic chlorinated compounds could be detected when the solids recovered at 10 and 20 min were pyrolyzed. The formation of aromatic hydrocarbons, especially benzene, also decreased for the solids recovered at longer times. It was also noted that lignin-derivable compounds were not produced during pyrolysis of any of the solids, despite that the FTIR results described above clearly showed the lignin origin in the solids. Thus, it is likely that the interaction between the dechlorinated PVC hydrocarbons and lignin of red oak in the HCl-containing solutions led to the formation of highly condensed aromatic structures containing highly stable intermolecular C-C and C-O bonds.

3.2.4. SEM results

In Fig. 6, the microstructures of the solids recovered during the co-conversion using a 1:1 ratio of red oak to PVC at 280 °C are compared with untreated red oak, as well as the red oak converted in the same temperature GVL for 40 min in the absence of PVC. The original plant structure was clearly observed in the red oak converted without PVC. In comparison, the plant structures were completely lost in the solids recovered from the co-conversion of red oak and PVC. Rather, the solids had highly condensed and uniform microstructures. During the co-conversion, the plant wall structure was destroyed due to the dissolution of the carbohydrates in the solvent catalyzed by the PVC-derived HCl. While the carbohydrates further decomposed to become smaller molecules, thermally stable lignin and dechlorinated PVC hydrocarbons reacted with each other to form condensed solid products.

3.2.5. Elemental analysis results

Elemental analysis results of the solids recovered from the co-conversion, and the red oak converted in GVL in the absence of PVC are given in Table S4. The reaction conditions for recovering the solids were selected to make sure that the chlorine-associated FTIR bands were absent in these solids (Fig. 4 and Figure S6). Compared to the red oak converted without PVC, the solids recovered from the co-conversion had significantly higher carbon content and reduced oxygen content. When the solids recovered at different reaction times using a 1:1 ratio of red oak to PVC were compared with each other, C and H contents in the solids increased whereas O content decreased with increasing reaction time. The HHVs were 27.27 MJ/kg, 32 MJ/kg, and 34.31 MJ/kg for the solids recovered after 10, 15 and 20 mins, respectively. The same increasing and decreasing trends of C, H, and O were also observed among the solids recovered at the same reaction time (20 min) but using higher PVC loadings. The HHVs of the solids recovered using 2:1 and 1:1 ratios of red oak and PVC were 28.63 MJ/kg and 34.31 MJ/kg. The maximum HHV of 36.32 MJ/kg was obtained with the solid recovered using a 2:3 ratio of red oak and PVC, which is even higher than the HHV of anthracite coal (i.e., 30.08 MJ/kg, Standard grade coal). The high HHVs of the solids were attributed to both the PVC-originating hydrocarbons and the highly carbonized lignin-derived structures. A higher PVC loading in the feedstock would increase the relative content of PVC-originating hydrocarbons in the solids, thus increasing the HHV.

3.2.6. Chlorine distribution and chlorine product recovery

During co-conversion of red oak and PVC, PVC-derived HCl dissolved in the solution catalyzed red oak conversion. On the other hand, the transition of HCl to CA occurred in the solvent due to the secondary reaction of HCl. As described above, the presence of chlorine in the solids depends on the reaction conditions. In this study, the chlorine content in the solids was measured using the standard method described in the experimental section, and the organic chlorine content was calculated based on the concentration of CA in the reaction solution. Since no other organic chlorinated compounds were detected during the liquid analysis, the inorganic chlorine (Cl^-) in the solution could be determined by subtracting the organic chlorine in CA and the chlorine in the solids from the total chlorine contained in PVC. The distribution of chlorine among the products during the co-conversion at 280 °C using a 1:1 ratio of red oak to PVC is shown in Fig. 7 as a function of reaction time. After a 5 min reaction, chlorine presented in both the liquid and solid due to incomplete PVC dehydrochlorination. No chlorine was detected in the solids recovered after 10 min or longer reaction times. These results are consistent with the results of the solid analysis described above. Due to the secondary reaction of HCl to CA, the organic chlorine content increased with increasing reaction time. After a 25 min reaction, 82% of total chlorine remained as Cl^- and the rest 18% presented in the form of CA.

It is noteworthy that CA is a functional monomer that has wide medical uses. For example, it can be used to derivatize L-hydroxyproline, a diagnostic marker of bone turnover and liver fibrosis. In this study, carbohydrate-derived products are water-soluble, whereas CA is water-insoluble. Therefore, water was added to the post-reaction solution to precipitate CA crystals as shown in Figure S7. In the GC/MS chromatogram of the precipitate shown in Figure S8, the sole major peak was CA. The purity of CA in the precipitate was determined to be 91.2%.

3.2.7. Proposed reaction mechanism

The reaction mechanism of red oak and PVC co-conversion in GVL is illustrated in Fig. 8. At the initial stage of the reaction, rapid dehydrochlorination of PVC releases HCl. The *in-situ* generated HCl in the solution then catalyzes depolymerization and dehydration of cellulose and hemicellulose to produce LGO and FF as the major monomers (Mamman et al., 2008; He et al., 2017). On the other hand, the dechlorinated PVC hydrocarbons and carbohydrate-free lignin further reacts with each other to form a highly condensed aromatic structure containing alkyl linkages. While the majority of chlorine in PVC is transformed into Cl^- ions in the solution, the rest is utilized to form CA.

4. Conclusions

A novel approach was developed to convert PVC-containing wastes. During co-conversion of red oak and PVC in GVL, HCl generated from dehydrochlorination of PVC served as an acid catalyst to promote red oak conversion to valuable chemicals. Up to 84.1% of liquid products, 14.4% of LGO, and 14.3 % of FF were obtained during the PVC aid conversion of biomass. It also showed that, the dechlorinated PVC hydrocarbons reacted with red oak-derived lignin in the solvent to form chlorine-free solids with high thermal stability. The HHV of the solids was up to 36.32 MJ/kg, and thus they can be used as high-quality, clean fuels. During the co-conversion, more than 80% of PVC chlorine was transformed into Cl^- ions, and the rest formed CA. Crystalized CA was recovered from the post-reaction solvent with a purity of 91.2%.

Declaration of Competing Interest

The authors declare that they have no known competing financial interests or personal relationships that could have appeared to influence

the work reported in this paper.

Acknowledgment

The research is supported by the National Science Foundation (grants no. 1803823 &
1826978).

Appendix A. Supplementary data

Supplementary data to this article can be found online at https://doi.org/10.1016/j.wasman.2022.04.018.

References

A, L., Radhakrishnan, H., Hu, H., Bai, X., 2021. One-pot production of oxygenated monomers and selectively oxidized lignin from biomass based on plasma electrolysis. Green Chem. 23, 9109–9125. doi:10.1039/d1gc03315h.

Ali, M.F., Siddiqui, M.N., 2005. Thermal and catalytic decomposition behavior of PVC mixed plastic waste with petroleum residue. J. Anal. Appl. Pyrol. 74, 282–289. https://doi.org/10.1016/j.jaap.2004.12.010.

Arena, U., 2012. Process and technological aspects of municipal solid waste gasification. A review. Waste Manage. 32, 625–639. https://doi.org/10.1016/j.wasman.2011.09.025.

Bockhorn, H., Hentschel, J., Hornung, A., Hornung, U., 1999. Environmental engineering: Stepwise pyrolysis of plastic waste. Chem. Eng. Sci. 54, 3043–3051. https://doi.org/10.1016/s0009-2509(98)00385-6.

Braden, J., Bai, X., 2018. Production of biofuel precursor chemicals from the mixture of cellulose and polyvinylchloride in polar aprotic solvent. Waste Manage. 78, 894–902. https://doi.org/10.1016/j.wasman.2018.07.011.

Braun, D., 2002. Recycling of PVC. Prog. Polym. Sci. 27, 2171–2195. https://doi.org/10.1016/s0079-6700(02)00036-9.

Brebu, M., Vasile, C., 2010. Thermal degradation of lignin-a review. Cellul. Chem. Technol. 44 (9), 353–363.

Cao, F., Schwartz, T.J., McClelland, D.J., Krishna, S.H., Dumesic, J.A., Huber, G.W., 2015. Dehydration of cellulose to levoglucosenone using polar aprotic solvents. Energy Environ. Sci. 8, 1808–1815. https://doi.org/10.1039/c5ee00353a.

Cesprini, E., Resente, G., Causin, V., Urso, T., Cavalli, R., Zanetti, M., 2020. Energy recovery of Glued Wood Waste – a review. Fuel 262, 116520. https://doi.org/10.1016/j.fuel.2019.116520.

Chen, X., Luo, Y., Bai, X., 2021. Upcycling polyamide containing post-consumer tetra pak carton packaging to valuable chemicals and recyclable polymer. Waste Manage. 131, 423–432. https://doi.org/10.1016/j.wasman.2021.06.031.

Comba, M.B., Tsai, Y.-H., Sarotti, A.M., Mangione, M.I., Suárez, A.G., Spanevello, R.A., 2018. Levoglucosenone and its new applications: Valorization of cellulose residues. Eur. J. Org. Chem. 2018, 590–604. https://doi.org/10.1002/ejoc.201701227.

Danthurebandara, M., Van Passel, S., Vanderreydt, I., Van Acker, K., 2015. Assessment of environmental and economic feasibility of Enhanced Landfill Mining. Waste Manage. 45, 434–447. https://doi.org/10.1016/j.wasman.2015.01.041.

Decker, C., 1976. Oxidative degradation of poly(vinyl chloride). J. Appl. Polym. Sci. 20, 3321–3336. https://doi.org/10.1002/app.1976.070201213.

Decker, C., 1984. Photodegradation of PVC. In: Owen, E.D. (Ed.), Degradation and Stabilisation of PVC. Springer Netherlands, Dordrecht, pp. 81–136. https://doi.org/10.1007/978-94-009-5618-6_3.

Dias, A.S., Lima, S., Pillinger, M., Valente, A.A., 2010. Furfural and furfural-based Industrial Chemicals. Ideas Chem. Mol. Sci. 165–186 https://doi.org/10.1002/9783527630554.ch8.

EPA, 2021. National Overview: Facts and Figures on Materials. Wastes and Recycling, archived at http://web.archive.org/ web/20210304173859/https://www.epa.gov/factsand-figures-about-materials-waste-and-recycling/ national-overview-facts-and-figures-materials.

Eseyin, A.E., Steele, P.H., 2015. An overview of the applications of furfural and its derivatives. Int. J. Adv. Chem. 3, 42. https://doi.org/10.14419/ijac.v3i2.5048.

Ghosh, A., Bai, X., Brown, R.C., 2018. Solubilized carbohydrate production by acid-catalyzed depolymerization of cellulose in polar aprotic solvents. ChemistrySelect 3, 4777–4785. https://doi.org/10.1002/slct.201800764.

Ghosh, A., Brown, R.C., Bai, X., 2016. Production of solubilized carbohydrate from cellulose using non-catalytic, supercritical depolymerization in polar aprotic solvents. Green Chem. 18, 1023–1031. https://doi.org/10.1039/c5gc02071a.

Hameed, Z., Aslam, M., Khan, Z., Maqsood, K., Atabani, A.E., Ghauri, M., Khurram, M.S., Rehan, M., Nizami, A.-S., 2021. Gasification of municipal solid waste blends with biomass for energy production and resources recovery: Current status, Hybrid Technologies and innovative prospects. Renew. Sustain. Energy Rev. 136, 110375 https://doi.org/10.1016/j.rser.2020.110375.

He, J., Liu, M., Huang, K., Walker, T.W., Maravelias, C.T., Dumesic, J.A., Huber, G.W., 2017. Production of levoglucosenone and 5-hydroxymethylfurfural from cellulose in polar aprotic solvent–water mixtures. Green Chem. 19, 3642–3653. https://doi.org/10.1039/c7gc01688c.

Helsen, L., Van den Bulck, E., 2005. Review of Disposal Technologies for chromated copper arsenate (CCA) treated wood waste, with detailed analyses of thermochemical conversion processes. Environ. Pollut. 134, 301–314. https://doi.org/10.1016/j.envpol.2004.07.025.

Hu, B., Lu, Q., Wu, Y.-T., Xie, W.-L., Cui, M.-S., Liu, J.i., Dong, C.-Q., Yang, Y.-P., 2020. Insight into the formation mechanism of levoglucosenone in phosphoric acid-catalyzed fast pyrolysis of cellulose. J. Energy Chem. 43, 78–89. https://doi.org/10.1016/j.jechem.2019.08.001.

Huang, Q., Tang, Y., Wang, S., Chi, Y., Yan, J., 2016. Effect of cellulose and polyvinyl chloride interactions on the catalytic cracking of tar contained in Syngas. Energy Fuels 30, 4888–4894. https://doi.org/10.1021/acs.energyfuels.6b00432.

Inoue, T., Miyuki, M., Kamitani, M., Kano, J., Saito, F., 2005. Dechlorination of polyvinyl chloride by its grinding with Koh and Naoh. Adv. Powder Technol. 16, 27–34. https://doi.org/10.1163/1568552053166638.

Jiang, J., Shi, K.e., Zhang, X., Yu, K., Zhang, H., He, J., Ju, Y., Liu, J., 2022. From plastic waste to wealth using chemical recycling: A review. J. Environ. Chem. Eng. 10, 106867. https://doi.org/10.1016/j.jece.2021.106867.

Kabbour, M., Luque, R., 2020. Furfural as a platform chemical. Biomass, Biofuels, Biochem. 283–297 https://doi.org/10.1016/b978-0-444-64307-0.00010-x.

Kawamoto, H., Saito, S., Hatanaka, W., Saka, S., 2007. Catalytic pyrolysis of cellulose in sulfolane with some acidic catalysts. J. Wood Sci. 53, 127–133. https://doi.org/10.1007/s10086-006-0835-y.

Kim, J.-Y., Oh, S., Park, Y.-K., 2020. Overview of biochar production from preservative-treated wood with detailed analysis of biochar characteristics, heavy metals behaviors, and their ecotoxicity. J. Hazard. Mater. 384, 121356 https://doi.org/10.1016/j.jhazmat.2019.121356.

Kollikkathara, N., Feng, H., Yu, D., 2010. A system dynamic modeling approach for evaluating municipal solid waste generation, landfill capacity and related cost management issues. Waste Manage. 30, 2194–2203. https://doi.org/10.1016/j.wasman.2010.05.012.

Krzymien, M.E., 1997. PVC photo-oxidative degradation: Identification of volatiles. Macromol. Symp. 115, 27–40. https://doi.org/10.1002/masy.19971150104.

Kumar, A., Sharma, M.P., 2014. Estimation of GHG emission and energy recovery potential from MSW landfill sites. Sustainable Energy Technol. Assess. 5, 50–61. https://doi.org/10.1016/j.seta.2013.11.004.

Kuramochi, H., Nakajima, D., Goto, S., Sugita, K., Wu, W., Kawamoto, K., 2008. HCl emission during co-pyrolysis of Demolition Wood with a small amount of PVC film and the effect of wood constituents on HCl emission reduction. Fuel 87, 3155–3157. https://doi.org/10.1016/j.fuel.2008.03.021.

Sarotti, A.M., Zanardi, M., Spanevello, R.A., 2012. Recent applications of levoglucosenone as chiral synthon. Curr. Organic Synth. 9, 439–459. https://doi.org/10.2174/157017912802651401.

Machado, G., Leon, S., Santos, F., Lourega, R., Dullius, J., Mollmann, M.E., Eichler, P., 2016. Literature review on furfural production from lignocellulosic biomass. Nat. Resour. 07, 115–129. https://doi.org/10.4236/nr.2016.73012.

Mamman, A.S., Lee, J.-M., Kim, Y.-C., Hwang, I.T., Park, N.-J., Hwang, Y.K., Chang, J.-S., Hwang, J.-S., 2008. Furfural: Hemicellulose/xylosederived biochemical. Biofuels, Bioprod. Biorefin. 2, 438–454. https://doi.org/10.1002/bbb.95.

McNeill, I.C., Memetea, L., Cole, W.J., 1995. A study of the products of PVC thermal degradation. Polym. Degrad. Stab. 49, 181–191. https://doi.org/10.1016/0141-3910(95)00064-s.

Mukherjee, S., Mukhopadhyay, S., Hashim, M.A., Sen Gupta, B., 2014. Contemporary environmental issues of landfill leachate: Assessment and remedies. Crit. Rev. Environ. Sci. Technol. 45, 472–590. https://doi.org/10.1080/10643389.2013.876524.

Polprasert, C., 2007. Organic Waste Recycling. Amer Welding Society.

Queiroz, A., Pedroso, G.B., Kuriyama, S.N., Fidalgo-Neto, A.A., 2020. Subcritical and supercritical water for chemical recycling of plastic waste. Curr. Opin. Green Sustainable Chem. 25, 100364 https://doi.org/10.1016/j.cogsc.2020.100364.

Raheem, A.B., Noor, Z.Z., Hassan, A., Abd Hamid, M.K., Samsudin, S.A., Sabeen, A.H., 2019. Current developments in chemical recycling of post-consumer polyethylene terephthalate wastes for new materials production: A review. J. Cleaner Prod. 225, 1052–1064. https://doi.org/10.1016/j.jclepro.2019.04.019.

Sadat-Shojai, M., Bakhshandeh, G.-R., 2011. Recycling of PVC Wastes. Polym. Degrad. Stab. 96, 404–415. https://doi.org/10.1016/j.polymdegradstab.2010.12.001.

Schyns, Z.O., Shaver, M.P., 2020. Mechanical recycling of Packaging Plastics: A Review. Macromol. Rapid Commun. 42, 2000415. https://doi.org/10.1002/marc.202000415.

Shahidul, M.I., Malcolm, M.L., Hashmi, M.S.J., Alhaji, M.H., 2020. Waste Resources recycling in achieving economic and environmental sustainability: Review on Wood Waste Industry. Encyclopedia Renew. Sustain. Mater. 965–974 https://doi.org/10.1016/b978-0-12-803581-8.11275-5.

Shen, Y., Yu, S., Ge, S., Chen, X., Ge, X., Chen, M., 2017. Hydrothermal carbonization of medical wastes and lignocellulosic biomass for solid fuel production from lab-scale to pilot-scale. Energy 118, 312–323. https://doi.org/10.1016/j.energy.2016.12.047.

Song, Z., Xiu, F.-R., Qi, Y., 2022. Degradation and partial oxidation of waste plastic express packaging bags in supercritical water: Resources transformation and pollutants removal. J. Hazard. Mater. 423, 127018 https://doi.org/10.1016/j.jhazmat.2021.127018.

Srivastava, A.N., Chakma, S., 2020. Quantification of landfill gas generation and energy recovery estimation from the municipal solid waste landfill sites of Delhi, India. Energy Sources, Part A: Recov., Util., Environ. Effects 1–14. https://doi.org/10.1080/15567036.2020.1754970.

Standard grade coal. Engineering Tool Box. URL https://www.engineeringtoolbox.com/coal-heating-values-d_1675.html.

Stromberg, R.R., Straus, S., Achhammer, B.G., 1959. Thermal decomposition of poly (vinyl chloride). J. Polym. Sci. 35, 355–368. https://doi.org/10.1002/pol.1959.1203512904.

Tamanna, K., Raman, S.N., Jamil, M., Hamid, R., 2020. Utilization of wood waste ash in Construction Technology: A Review. Constr. Build. Mater. 237, 117654 https://doi.org/10.1016/j.conbuildmat.2019.117654.

Tang, C., Wang, Y.-Z., Zhou, Q., Zheng, L., 2003. Catalytic effect of Al–Zn composite catalyst on the degradation of PVC-containing polymer mixtures into pyrolysis oil. Polym. Degrad. Stab. 81, 89–94. https://doi.org/10.1016/s0141-3910(03)00066-1.

Titow, W.V., 1999. PVC plastics: properties, processing, and applications. Springer Netherlands, Dordrecht.

Thiounn, T., Smith, R.C., 2020. Advances and approaches for chemical recycling of plastic waste. J. Polym. Sci. 58, 1347–1364. https://doi.org/10.1002/pol.20190261.

Vaverková, M.D., 2019. Landfill impacts on the environment— review. Geosciences 9, 431. https://doi.org/10.3390/geosciences9100431.

Wang, Z., Burra, K.G., Lei, T., Gupta, A.K., 2021. Co-pyrolysis of waste plastic and solid biomass for synergistic production of biofuels and chemicals-A Review. Prog. Energy Combust. Sci. 84, 100899 https://doi.org/10.1016/j.pecs.2020.100899.

Wei, X., Wang, Z., Wu, Y., Yu, Z., Jin, J., Wu, K., 2014. Fast pyrolysis of cellulose with solid acid catalysts for levoglucosenone. J. Anal. Appl. Pyrol. 107, 150–154. https://doi.org/10.1016/j.jaap.2014.02.015.

Xiu, F.-R., Wang, Y., Yu, X., Li, Y., Lu, Y., Zhou, K., He, J., Song, Z., Gao, X., 2020. A novel safety treatment strategy of DEHP-rich flexible polyvinyl chloride waste through low-temperature critical aqueous ammonia treatment. Sci. Total Environ. 708, 134532 https://doi.org/10.1016/j.scitotenv.2019.134532.

Xue, Y., Bai, X., 2018. Synergistic enhancement of product quality through fast co-pyrolysis of acid pretreated biomass and waste plastic. Energy Convers. Manage. 164, 629–638. https://doi.org/10.1016/j.enconman.2018.03.036.

Xue, Y., Johnston, P., Bai, X., 2017. Effect of catalyst contact mode and gas atmosphere during catalytic pyrolysis of waste plastics. Energy Convers. Manage. 142, 441–451. https://doi.org/10.1016/j.enconman.2017.03.071.

Xue, Y., Kelkar, A., Bai, X., 2016. Catalytic co-pyrolysis of biomass and polyethylene in a tandem micropyrolyzer. Fuel 166, 227–236. https://doi.org/10.1016/j.fuel.2015.10.125.

Xue, Y., Zhou, S., Brown, R.C., Kelkar, A., Bai, X., 2015. Fast pyrolysis of biomass and waste plastic in a fluidized bed reactor. Fuel 156, 40–46. https://doi.org/10.1016/j.fuel.2015.04.033.

Yu, J., Sun, L., Ma, C., Qiao, Y., Yao, H., 2016. Thermal degradation of PVC: A Review. Waste Manage. 48, 300–314. https://doi.org/10.1016/j.wasman.2015.11.041.

Zanardi, M.M., Suárez, A.G., 2009. Synthesis of a simple chiral auxiliary derived from levoglucosenone and its application in a diels–alder reaction. Tetrahedron Lett. 50, 999–1002. https://doi.org/10.1016/j.tetlet.2008.12.048.

Zhang, M., Buekens, A., Jiang, X., Li, X., 2015. Dioxins and polyvinylchloride in combustion and fires. Waste Manage. Res.: J. Sustain. Circ. Economy 33, 630–643. https://doi.org/10.1177/0734242x15590651.

Zhou, H., Wu, C., Onwudili, J.A., Meng, A., Zhang, Y., Williams, P.T., 2015. Effect of interactions of PVC and biomass components on the formation of polycyclic aromatic hydrocarbons (PAH) during fast co-pyrolysis. RSC Adv. 5, 11371–11377. https://doi.org/10.1039/c4ra10639c.